

Article

The Compressive Properties and Deformation Mechanism of Closed-Cell Aluminum Foam with High Porosity after High-Temperature Treatment

Hu Zhang ^{1,2}, Mingfeng Lei ^{1,2} , Zanquan Lin ^{1,2}, Weipeng Gong ³, Jiajia Shen ⁴ and Yunbo Zhang ^{1,2,*}¹ School of Civil Engineering, Central South University, Changsha 410075, China² MOE Key Laboratory of Engineering Structures of Heavy Haul Railway, Central South University, Changsha 410075, China³ Shandong High-Speed High-Tech Materials Technology Co., Ltd., Jinan 250013, China⁴ Shandong Provincial Communications Planning and Design Institute Group Co., Ltd., Jinan 250031, China

* Correspondence: 204811045@csu.edu.cn

Abstract: As a new type of structurally functional material, aluminum foam is widely used in civil engineering due to its excellent noise and energy reduction, thermal insulation, and fire protection properties. However, systematic research into the mechanical properties, application technology, and specification standards of aluminum foam materials in civil engineering application scenarios is lacking. In this work, a special experimental study on the mechanical properties and deformation mechanism of closed-cell aluminum foam materials in compression after fire was carried out. The mechanism of deformation and failure of closed-cell aluminum foam was revealed, and the variation in the mechanical properties of closed-cell aluminum foam with porosity, and heating temperature were investigated. On the basis of the experimental results, the correlation function between material parameters and material porosity in the Liu-Subhash constitutive model was established through multiparameter regression analysis. Then, an intrinsic structure model of aluminum foam that can consider porosity was proposed. The research results show that (1) the compression deformation process of closed-cell aluminum foam specimens exhibits significant stage characteristics: a quasi-elastic stage of quasi-elastic deformation of the matrix and cell structure → a plateau stage of cell structure destabilization and damage → a densification stage of cell collapse and stacking. (2) As the porosity decreases, the aluminum foam material becomes more resistant to compressive deformation and shows better compressive mechanical properties overall. With an increase in the heat treatment temperature, the elastic gradient, compressive proof strength, and plateau stress of the aluminum foam material show a small decrease in the overall trend. (3) The predicted values of the intrinsic structure model of closed-cell aluminum foam are in good agreement with the experimental results, indicating that the model can efficiently characterize the stress-strain process of the material and is referable.

Keywords: closed-cell aluminum foam; temperature; mechanical properties; deformation mechanism

Citation: Zhang, H.; Lei, M.; Lin, Z.; Gong, W.; Shen, J.; Zhang, Y. The Compressive Properties and Deformation Mechanism of Closed-Cell Aluminum Foam with High Porosity after High-Temperature Treatment. *Sustainability* **2022**, *14*, 9850. <https://doi.org/10.3390/su14169850>

Academic Editor: Antonio Formisano

Received: 8 June 2022

Accepted: 4 August 2022

Published: 10 August 2022

Publisher's Note: MDPI stays neutral with regard to jurisdictional claims in published maps and institutional affiliations.



Copyright: © 2022 by the authors. Licensee MDPI, Basel, Switzerland. This article is an open access article distributed under the terms and conditions of the Creative Commons Attribution (CC BY) license (<https://creativecommons.org/licenses/by/4.0/>).

1. Introduction

Tunnels are an important part of high-grade highways and are affected by their semi-enclosed structure. On the one hand, the noise convergence during vehicle traffic is strong, and the sound pollution is serious [1]. On the other hand, once a fire accident occurs, it will not only endanger the lives of the drivers and passengers inside the tunnel but also cause damage to the tunnel structure. Therefore, improving the noise environment and preventing fire damage are important elements to realize high-quality service of highway tunnels in the new era. Aluminum foam, as a new type of material integrating structure and functionalization, has excellent energy absorption, vibration damping, sound absorption [2,3], thermal insulation [4,5], and electromagnetic shielding properties and has been widely

used in military and industrial fields [6,7]. Moreover, there have been considerable research results on the preparation techniques [8–11] and mechanical properties [12–14] and the constitutive relationship [15–17] of their materials in the corresponding scenarios. For example, Cowie and Itrausquin [18,19] investigated the microstructural characteristics and damage modes of aluminum foam after impact through dynamic impact experiments. Liu and Subhash [20] proposed a multi-parameter phenomenological model subjected to large deformations, which fully reflects the stage characteristics of structural foams in the process of compression deformation. Xi et al. [21] compared the variation function of the five parameters of the Liu–Subhash model with temperature based on the experimental results and established a static compression constitutive model for aluminum foam considering the effect of temperature.

In recent years, aluminum foam materials have also attracted the attention of civil engineering practitioners due to their excellent performance in noise reduction, energy absorption, heat insulation, and fire prevention. The majority of engineers have made active attempts to apply the materials to various infrastructure projects, and there are now several application test sites. However, in general, the application of aluminum foam materials in civil engineering is still in the exploration and testing stage, and there is still a lack of large-scale promotion and application. The fundamental reason is that as these are application innovation class materials, there is still a lack of systematic research on the mechanical properties, application technology, and specification standards in civil engineering application scenarios. For example, when aluminum foam is used as a fireproof material in tunnel engineering, what are the mechanical properties of the material after a fire? Few targeted results have been reported.

To this end, this paper focuses on the application scenario of aluminum foam in tunneling. Special experimental research on the compressive mechanical properties and deformation mechanism of aluminum foam materials after fire is carried out. Furthermore, a quasi-static compressive constitutive model of aluminum foam considering porosity based on the Liu–Subhash model was established by fitting the experimental data.

2. Design of the Experiment

2.1. Sample Preparation

A closed-cell aluminum foam material of 1060 aluminum was selected for the test, which was made by Shandong High-speed High-tech Materials Technology Company by the melt foaming method, with a porosity of 84.3%, 90.1%, 91.0%, and 94.1%, and the average cell size was 5 mm. During the preparation of the sample, it was processed and shaped by wire cutting, and the specimen size was 50 mm × 50 mm × 75 mm, as shown in Figure 1.



Figure 1. Aluminum foam samples.

2.2. High-Temperature Treatment of Specimens

The aluminum foam specimens were placed into an SX-B16103 chamber electric furnace for high-temperature treatment. In the test, five temperature conditions were considered in turn: 700 °C (exceeding the melting point of metallic aluminum), 600 °C, 400 °C, 100 °C, and 25 °C (no heating), with three specimens under each temperature condition. The specific heating system is shown in Figure 2. During the heat treatment, the aluminum foam specimens were first heated to the corresponding temperature, held for 3 h, and then the heating ended and the specimens cooled naturally to room temperature.

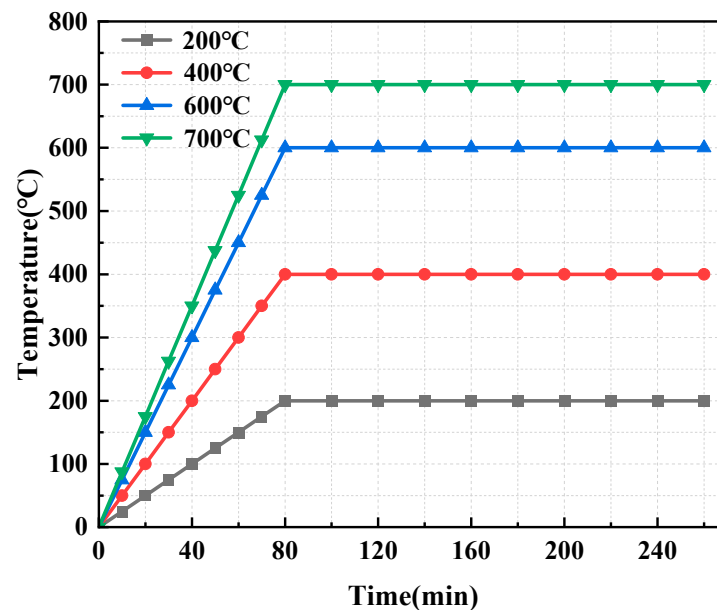


Figure 2. Heating curve of aluminum foam.

2.3. Quasi-Static Compression Experiment

Quasi-static compression experiments were carried out sequentially after the high-temperature treatment. The test platform was a WDW-50 microcomputer-controlled electrohydraulic servo universal testing machine, the set loading rate was 5 mm/min, the control mode was displacement control, and the test indices were the loading force and compression displacement. The test system is shown in Figure 3.

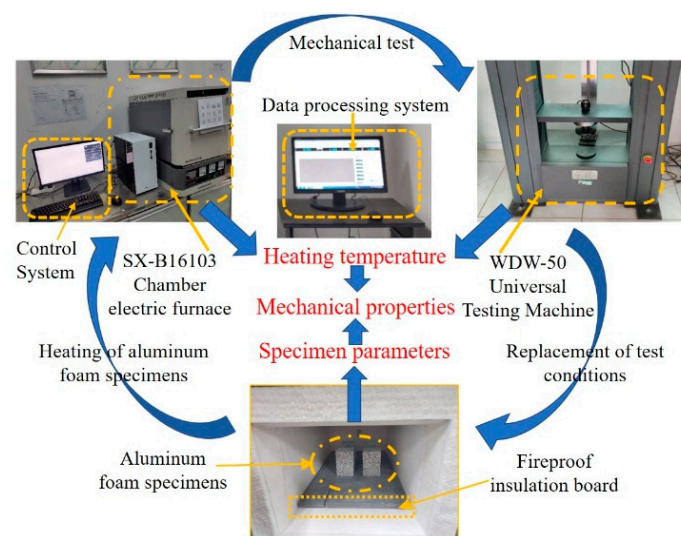


Figure 3. Test system.

3. Experimental Results and Analysis

3.1. Compression Deformation Process Analysis

Figures 4 and 5 show the state changes of the aluminum foam sample in the whole process of the quasi-static compression test, from which we obtained the following results:

- (1) When the load is small (the strain is less than 0.05), the cell structure of aluminum foam mainly deforms by elastic bending. However, the cell structure remains intact, and the structure does not fail. The cell structure's form can recover in time after unloading, as depicted in Figure 4a,b.
- (2) As the load increases, and when the stress exceeds the compressive proof strength of the aluminum foam's cell wall, the aluminum matrix undergoes plastic deformation. The cell structure cracks and expands, forming a yield zone, as shown in Figures 4c and 5a.
- (3) With the further increase in the compression load, a larger range of yield zones appear in the aluminum foam's cell wall structure, and part of the cell structure collapses, as shown in Figure 4d,e. Thereafter, the aluminum foam's cell collapses in a large volume, as illustrated in Figure 4f,g. The cell structure is completely destroyed and compacted, and the cell walls start to stack and squeeze each other, as presented in Figure 5b. Owing to the complete disappearance of cells, the compression process ends, and the force characteristics enter the densification stage from the plateau stage, with a subsequent rapid increase in stress.

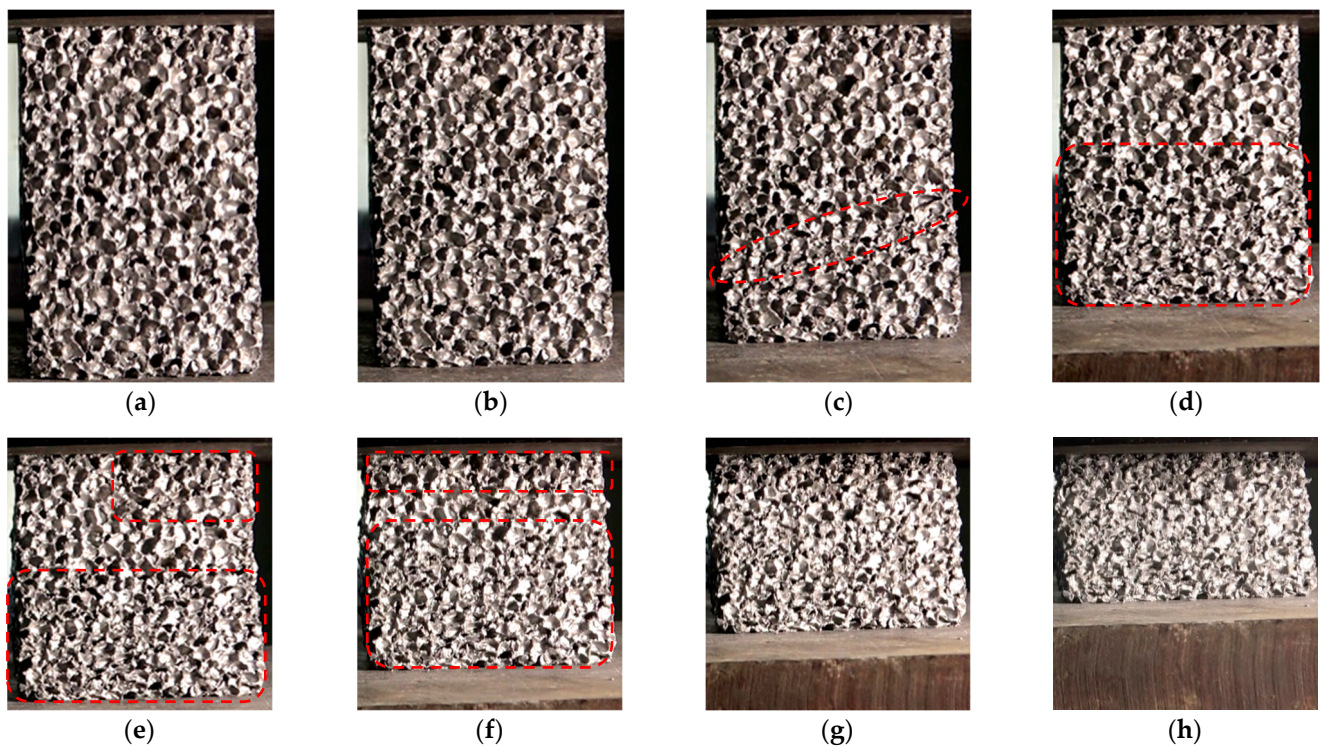


Figure 4. Compression deformation process of closed-cell aluminum foam: (a) $\varepsilon = 0$ initial stage, (b) $\varepsilon = 0.05$ elastic bending deformation of cells, (c) $\varepsilon = 0.1$ crack generation, (d) $\varepsilon = 0.2$ collapse zone appears, (e) $\varepsilon = 0.3$ large-scale collapse, (f) $\varepsilon = 0.4$ collapse zone is fully formed, (g) $\varepsilon = 0.5$ cells are completely destroyed, and (h) $\varepsilon = 0.6$ aluminum substrate stacking and pressing.

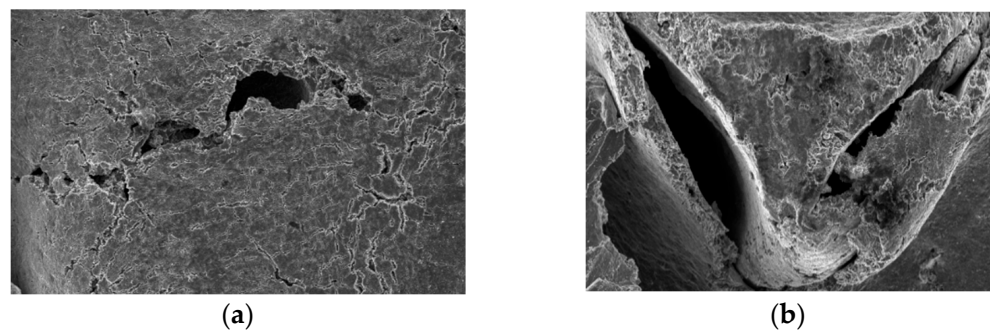


Figure 5. SEM images of aluminum foam's cells: (a) $\varepsilon = 0.05$ local crack generation and (b) $\varepsilon = 0.5$ local aluminum matrix extrusion.

3.2. Stress–Strain Characteristics

The stress–strain curves of the closed-cell aluminum foam obtained from the quasi-static compression test are shown in Figure 6. From the deformation process analysis in Section 2.1, the compression deformation process of the aluminum foam specimens exhibits significant stage characteristics, for which the test results (Figure 6) can be further generalized to obtain the stress–strain characteristic curve, as shown in Figure 7.

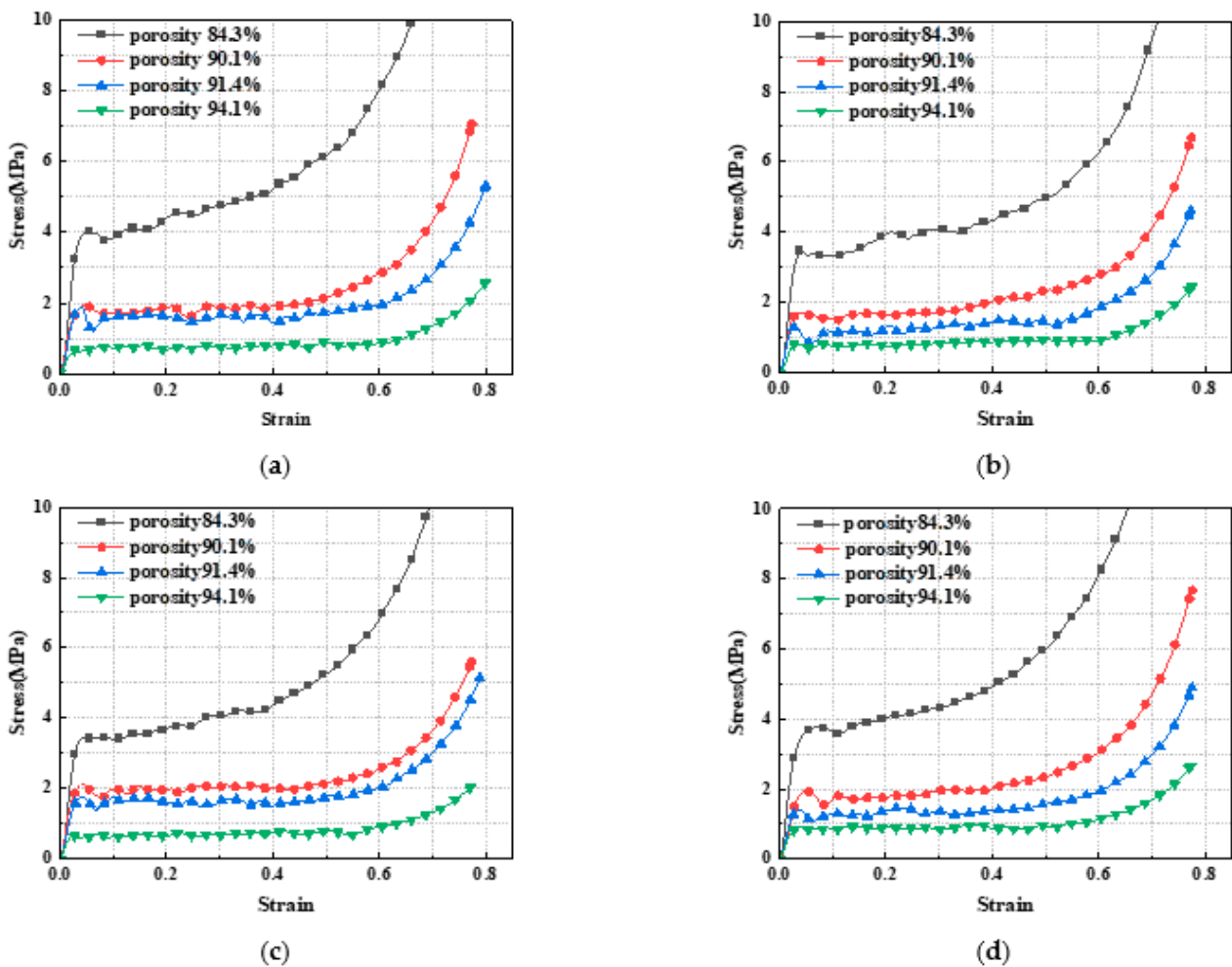


Figure 6. Uniaxial compressive stress–strain curve of aluminum foam: (a) 25 °C, (b) 200 °C, (c) 400 °C, and (d) 600 °C.

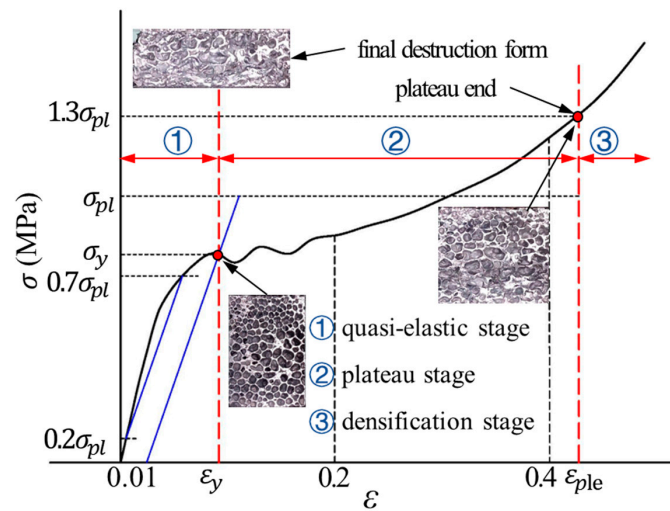


Figure 7. Calculation method of basic mechanical parameters.

- (1) Quasi-elastic stage: at the beginning of loading, the load is small, the aluminum foam matrix and the cell structure are mainly subjected to elastic deformation, the strain is small (less than 0.05), and the stress increases linearly.
- (2) Plateau stage: With the increase in force deformation of the aluminum foam matrix and cell structure, the aluminum foam’s cell structure is damaged, some cells crack and start to collapse, and the compression curve enters the plateau stage. In the compression process, the aluminum foam’s cells first produce bending yielding, and the cell wall structure does not immediately but slowly deforms until the cell space is completely compressed. At this stage (strain is in the range 0.05–0.5), with the increase in strain, the stress changes minimally, which reflects that the closed-cell aluminum foam material has strong energy absorption characteristics.
- (3) With the continuous collapse of the aluminum foam’s cells, the cells will be completely compacted, the aluminum foam matrix starts to stack densely on top of each other, and the compression curve enters the densification stage. In this stage, the stress rises sharply, and the slope of the tangent line of the stress–strain curve increases with the increase in strain.

3.3. Compression Mechanical Property Analysis

The basic mechanical parameters of the aluminum foam specimens at different stages can be calculated as follows (Figure 7), as shown in Table 1.

Table 1. Basic mechanical property parameters of aluminum foam.

T/°C	MPa	Porosity							
		84.3%		90.1%		91.4%		94.1%	
		Average Value	Standard Deviation						
25	E_s^1	134.03	6.919	88.58	0.009	75.67	2.976	23.15	3.561
	σ_y^2	3.69	0.102	1.86	0.120	1.55	0.105	0.54	0.067
	σ_{pl}^3	4.67	0.077	1.94	0.007	1.46	0.066	0.67	0.073
200	E_s^1	117.17	6.116	75.09	3.326	71.20	3.066	36.65	2.121
	σ_y^2	3.18	0.132	1.66	0.030	1.48	0.067	0.67	0.057
	σ_{pl}^3	4.03	0.011	1.81	0.034	1.48	0.059	0.73	0.062
400	E_s^1	122.12	6.133	81.36	4.646	61.62	2.957	28.13	1.895
	σ_y^2	3.18	0.149	1.88	0.092	1.47	0.078	0.57	0.047
	σ_{pl}^3	3.90	0.105	2.02	0.002	1.50	0.079	0.68	0.010
600	E_s^1	115.95	5.394	71.50	0.207	72.41	4.371	36.45	2.294
	σ_y^2	3.83	0.172	1.73	0.003	1.47	0.083	0.76	0.058
	σ_{pl}^3	4.85	0.282	1.98	0.069	1.49	0.102	0.78	0.069

¹ E_s : Elastic gradient, ² σ_y : Compressive proof strength, and ³ σ_{pl} : Plateau stress.

- (1) Elastic gradient (E_s): gradient of the elastic straight lines between stresses of 0.7- and 0.2-times plateau stress.
- (2) Compressive proof strength (σ_y): compressive stress at a plastic compressive strain of 0.01.
- (3) Plateau stress (σ_{pl}): arithmetical mean of the stresses at smaller strain intervals between 0.2 and 0.4 compressive strain.

From this analysis, the following findings are realized:

- (1) With an increase in the heat treatment temperature, the elastic gradient, compressive proof strength, and plateau stress of the aluminum foam material generally show a small decreasing trend. When the heating temperature is less than 600 °C, the compressive mechanical properties of the aluminum foam material decrease to a lesser extent. However, when the heating temperature reaches 700 °C, the structure of the closed-cell aluminum foam changes, the aluminum foam specimen is seriously deformed, and there is no experimental condition to complete the compression experiment.
- (2) After the aluminum foam is heated to 200 °C, 400 °C, and 600 °C, its mechanical parameters show a similar pattern, i.e., the mechanical parameters of aluminum foam materials with lower porosity perform better. The reason is that with a decrease in porosity, the aluminum matrix content of aluminum foam materials increases, the percentage of pore volume decreases, the thickness of each cell wall increases, and the resistance of aluminum foam specimens to compressive deformation is enhanced. They show better compressive mechanical properties overall.

4. Constitutive Model of Closed-Cell Aluminum Foam Based on Experiment

In 2004, Liu and Subhash studied and proposed a foam material constitutive model containing six parameters based on the stress–strain full process curves of metal foam materials [20]:

$$\sigma = P_1 \frac{e^{P_2 \varepsilon} - 1}{P_6 + e^{P_3 \varepsilon}} + e^{P_4} (e^{P_5 \varepsilon} - 1) \quad (1)$$

In the equation, σ is the stress, and ε is the strain. $P_i (i = 1, \dots, 6)$ are material parameters, where P_1 is the yield stress; P_2 and P_3 characterize the hardening properties of the plateau stage; P_4 and P_5 characterize the starting point of the densification stage and the rate of stress change in the densification stage, respectively; and P_6 characterizes the change in slope of the quasi-elastic stage.

Analysis of the above intrinsic structure model demonstrates that $P_i (i = 1, \dots, 6)$ are material constants. Liu and Subhash proposed to make $C_i = P_i (i = 1, \dots, 5)$, $P_6 = 1$. Then, Equation (1) can be further rewritten as follows:

$$\sigma = C_1 \frac{e^{C_2 \varepsilon} - 1}{1 + e^{C_3 \varepsilon}} + e^{C_4} (e^{C_5 \varepsilon} - 1) \quad (2)$$

In the equation, $C_i (i = 1, \dots, 5)$ are the combined material parameters.

The quasi-static stress–strain curves of aluminum foam with different porosity at room temperature are fitted to obtain the values of the intrinsic model parameters of aluminum foam materials with different porosity, as shown in Table 2 and Figure 8.

Table 2. Stress–strain curve fitting of aluminum foam specimens with different porosity at room temperature.

Porosity/%	C_1	C_2	C_3	C_4	C_5
84.3%	3.48	90.48	89.60	−5.31	10.28
90.1%	1.86	84.86	84.87	−6.41	10.21
91.4%	1.46	83.45	83.45	−7.28	10.91
94.1%	0.66	79.68	79.59	−9.01	11.81

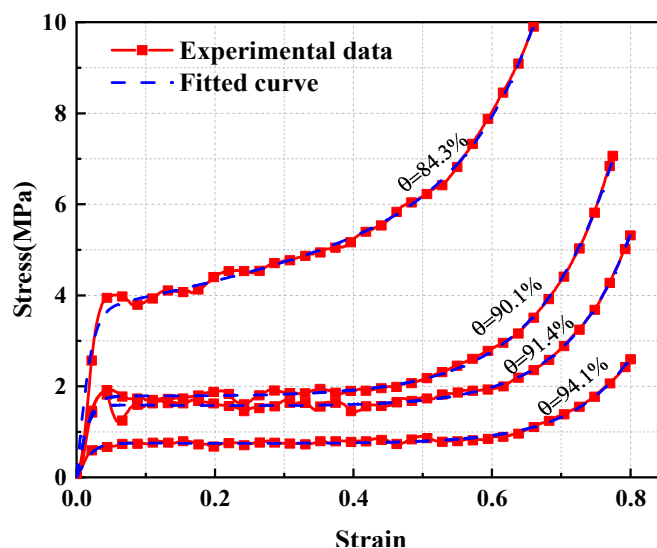


Figure 8. Stress–strain curves of aluminum foam specimens with different porosity at room temperature (25 °C).

From the analysis of Table 2 and Figure 9, the parameters $C_i (i = 1, \dots, 5)$ all exhibit variation characteristics related to the porosity of the specimen. Thus, these five parameters can be considered a function of porosity θ . On the basis of the aforementioned experimental results, a monotonic compression constitutive model of aluminum foam considering porosity can be obtained.

$$\sigma = C_1(\theta) \frac{e^{C_2(\theta)\epsilon} - 1}{1 + e^{C_3(\theta)\epsilon}} + e^{C_4(\theta)} (e^{C_5(\theta)\epsilon} - 1) \tag{3}$$

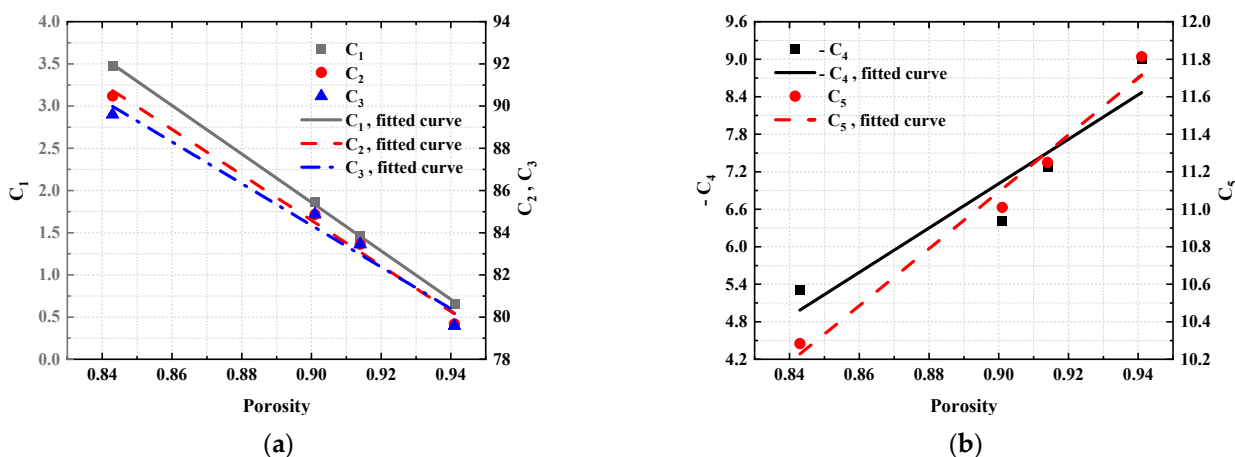


Figure 9. Variation law of each parameter with porosity: (a) C_1 , C_2 , and C_3 ; and (b) C_4 and C_5 .

In the equation, $C_i(\theta) (i = 1, \dots, 5)$ are the functions of porosity θ on the parameters of the aluminum foam material, which can be determined by fitting the experimental data. The fitting results of this test are shown in Equation (4) and Figure 9.

$$\begin{cases} C_1 = -28.7\theta + 27.7 \\ C_2 = -107.8\theta + 181.6 \\ C_3 = -98.8\theta + 173.3 \\ C_4 = -35.5\theta + 24.9 \\ C_5 = 15.2\theta - 2.6 \end{cases} \tag{4}$$

On the basis of the above constitutive model and its parameter values, the predicted stress–strain curves for the porosities of 85.1%, 90.0%, and 91.8% are given in Figure 10. The predicted results are in good agreement with the experimental results, indicating that the constitutive model of closed-cell aluminum foam established in this paper can efficiently characterize the stress–strain process of the material and is referable.

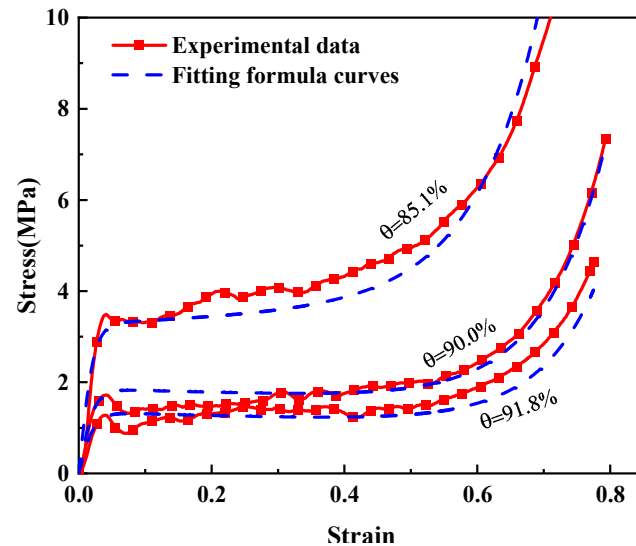


Figure 10. Comparison of the calculated results of the constitutive model and the experimental results of aluminum foam materials with different porosity at room temperature (25 °C).

5. Conclusions

- (1) Quasi-static compression performance tests on closed-cell aluminum foam materials after high-temperature treatment were carried out to reveal the mechanism of deformation failure of the materials. The results showed that the compressive deformation process of closed-cell aluminum foam specimens exhibited significant stage characteristics, namely, a quasi-elastic deformation stage of the aluminum foam matrix and cell structure → a plateau stage of the aluminum foam's cell structure destabilization and damage → a densification stage of the aluminum foam's cell collapse and stacking.
- (2) The variation law of the mechanical properties of closed-cell aluminum foam materials with porosity and heat treatment temperatures was obtained. That is, with a decrease in porosity, the aluminum matrix content of aluminum foam materials increased, the thickness of cell walls increased, and the resistance of aluminum foam specimens to compressive deformation was enhanced. They showed better compressive mechanical properties overall. With an increase in the heat treatment temperature, the elastic modulus, compressive proof strength, and plateau stress values of aluminum foam materials generally demonstrated a small decrease in the trend of change. When the heating temperature reached 700 °C, the closed-cell aluminum foam structure was completely destroyed.
- (3) A constitutive model of closed-cell aluminum foam materials considering porosity based on the experimental results was established. Likewise, in accordance with the experimental results, the correlation function between material parameters and porosity in the Liu–Subhash constitutive model was established using the method of multiparameter regression analysis. Then, a constitutive model of aluminum foam materials that can consider porosity was established. The validation results showed that the model predictions were in good agreement with the experimental results, indicating that the established modified constitutive model of closed-cell aluminum foam can efficiently characterize the stress–strain process of the material and is referable.

Author Contributions: Writing—original draft preparation, H.Z.; writing—review and editing, M.L.; experimentation, Z.L.; supervision, W.G. and J.S.; data curation, Y.Z.; project administration, W.G.; All authors have read and agreed to the published version of the manuscript.

Funding: This research was funded by the National Natural Science Foundation of China (No. 51978669), and the Natural Science Foundation of Hunan Province, China (No. 2021JJ30825) are gratefully acknowledged.

Data Availability Statement: The data used to support the findings of this study are available from the corresponding author upon request.

Acknowledgments: The authors express their sincere gratitude to all the reviewers for their comments devoted to improving the quality of this paper.

Conflicts of Interest: The authors declare that the research was conducted in the absence of any commercial or financial relationships that could be construed as potential conflicts of interest.

References

1. Zeng, S. Analysis of the influence of the characteristics of mountain soil and the noise in the tunnel on people: Active noise control system. *Arab. J. Geosci.* **2021**, *14*, 1–16.
2. Opiela, K.C.; Zielinski, T.G.; Dvorak, T.; Kudela, S., Jr. Perforated closed-cell aluminium foam for acoustic absorption. *Appl. Acoust.* **2021**, *174*, 107706. [\[CrossRef\]](#)
3. Lu, T.; Hess, A.; Ashby, M. Sound absorption in metallic foams. *J. Appl. Phys.* **1999**, *85*, 7528–7539. [\[CrossRef\]](#)
4. Navacerrada, M.A.; Fernandez, P.; Diaz, C.; Pedrero, A. Thermal and acoustic properties of aluminium foams manufactured by the infiltration process. *Appl. Acoust.* **2013**, *74*, 496–501. [\[CrossRef\]](#)
5. Ye, H.; Ma, M.; Ni, Q. An experimental study on mid-high temperature effective thermal conductivity of the closed-cell aluminum foam. *Appl. Therm. Eng.* **2015**, *77*, 127–133. [\[CrossRef\]](#)
6. Grilec, K.; Marić, G.; Miloš, K. Aluminium Foams in the Design of Transport Means. *J. Traffic Transp. Eng.* **2012**, *24*, 295–304. [\[CrossRef\]](#)
7. Dineshkumar, J.; Jesudas, T.; Elayaraja, R. Characteristics, applications and processing of aluminium foams—A Review. *Mater. Today Proc.* **2021**, *42*, 1773–1776. [\[CrossRef\]](#)
8. Singh, D.; Mittal, A.; Jain, V.; Gupta, D.; Singla, V.K. Investigations on Fabrication Techniques of Aluminium-Based Porous Material. *Adv. Manuf. Process.* **2019**, 219–227. [\[CrossRef\]](#)
9. Voronin, S.V.; Loboda, P.S.; Gorkunov, E.S.; Panin, V.E.; Ramasubbu, S. Methods for producing foamed aluminum. *AIP Conf. Proc.* **2017**, *1915*, 40064.
10. Karuppasamy, R.; Barik, D. Production methods of aluminium foam: A brief review. *Mater. Today Proc.* **2021**, *37*, 1584–1587. [\[CrossRef\]](#)
11. Rajak, D.K.; Kumaraswamidhas, L.A.; Das, S. Technical Overview of Aluminum Alloy Foam. *Rev. Adv. Mater. Sci.* **2017**, *49*, 68–86.
12. Haag, F.; Galio, A.; Schaeffer, L. Uniaxial compression tests of aluminium foams. *Proc. Inst. Mech Eng. Part B-J. Eng. Manuf.* **2002**, *216*, 633–636. [\[CrossRef\]](#)
13. Yamada, Y.; Banno, T.; Xie, Z.K.; Wen, C.E. Compressive Deformation Behaviour of a Closed-Cell Aluminum. *Mater. Sci. Forum.* **2006**, *510–511*, 150–153.
14. Ruan, D.; Lu, G.; Chen, F.; Siores, E. Compressive behaviour of aluminium foams at low and medium strain rates. *Compos. Struct.* **2002**, *57*, 331–336. [\[CrossRef\]](#)
15. Forest, S.; Blazy, J.S.; Chastel, Y.; Moussy, F. Continuum modeling of strain localization phenomena in metallic foams. *J. Mater. Sci.* **2005**, *40*, 5903–5910. [\[CrossRef\]](#)
16. Ding, Y.; Wang, S.; Zheng, Z.; Yang, L.; Yu, J. Dynamic crushing of cellular materials: A unique dynamic stress—Strain state curve. *Mech. Mater.* **2016**, *100*, 219–231. [\[CrossRef\]](#)
17. Zheng, Z.; Yu, J.; Wang, C.; Liao, S.; Liu, Y. Dynamic crushing of cellular materials: A unified framework of plastic shock wave models. *Int. J. Impact Eng.* **2013**, *53*, 29–43. [\[CrossRef\]](#)
18. Cowie, T.; Gurnham, C.W.A.; Braithwaite, C.H.; Lea, L.; Chau, R.; Germann, T.C.; Lane, J.M.D.; Brown, E.N.; Eggert, J.H.; Knudson, M.D. Impact performance of aluminium foams in a direct impact Hopkinson bar. *AIP Conf. Proc.* **2018**, *1979*, 110003.
19. Irausquin, I.; Perez-Castellanos, J.L.; Miranda, V.; Teixeira-Dias, F. Evaluation of the effect of the strain rate on the compressive response of a closed-cell aluminium foam using the split Hopkinson pressure bar test. *Mater. Des.* **2013**, *47*, 698–705. [\[CrossRef\]](#)
20. Liu, Q.; Subhash, G. A phenomenological constitutive model for foams under large deformations. *Polym. Eng. Sci.* **2004**, *44*, 463–473. [\[CrossRef\]](#)
21. Xi, H.; Liu, Y.; Tang, L.; Liu, Z.; Mu, J.; Yang, B. Constitutive model of aluminum foam with temperature effect under quasi-static compression. *J. Harbin Eng. Univ.* **2013**, *34*, 6.